

High Resolution Wind Retrieval from SeaWinds

David G. Long

Brigham Young University Microwave Earth Remote Sensing Laboratory

459 Clyde Building, Provo, UT 84602 USA

801-378-4383, FAX: 801-378-6586, e-mail: long@ee.byu.edu

Abstract—While originally designed for measuring vector winds over the ocean at a nominal resolution of 25 km, data from SeaWinds-on-QuikSCAT can be used to retrieve winds over the ocean at higher resolution with the aid of resolution enhancement reconstruction algorithms. This paper analyzes a technique for retrieving enhanced resolution winds at high resolution from SeaWinds data. Techniques for minimizing the required computation are described. As can be expected the wind estimates are noisier than standard resolution products. Some of the limitations of the approach and resulting products are considered. While validation of this approach to high resolution wind retrieval continues, the results thus far are very encouraging.

I. INTRODUCTION

The SeaWinds wind scatterometer was launched in 1999 on the QuikSCAT satellite. A second SeaWinds will be launched later this year onboard ADEOS-II. The Ku-band pencil-beam SeaWinds is designed to make nominally 25 km resolution observations of near-surface vector winds over the ocean. SeaWinds wind observations are currently being operationally used at various weather forecasting facilities where it has improved forecasting skill.

Like all radar scatterometers SeaWinds makes an indirect measurement of the wind. Its direct measurement is of the surface normalized radar backscatter (σ^o) from which the wind is retrieved with aid of a geophysical model function. SeaWinds σ^o measurements have proven useful in a variety of land and ice applications and are being operationally used for sea ice monitoring and iceberg tracking. SeaWinds land and ice applications have been aided by the use of resolution enhancement and reconstruction algorithms for which the SeaWinds sampling geometry is well-suited [1]. Recently, a new high resolution σ^o ocean product was introduced. This experimental operational product is actively being used to support hurricane and typhoon tracking.

Previous scatterometers have required multiple overlapping orbits to effectively apply the resolution enhancement techniques, precluding the use of the enhanced data for wind retrieval. However, the dense SeaWinds sampling enables the use of resolution enhancement for single-passes, albeit with degraded performance. It is thus possible to apply resolution enhancement techniques to the scatterometer backscatter measurements to enable retrieval at higher effective resolution than otherwise possible. In this paper a technique for retrieving enhanced resolution winds at high resolution (2.5 km sample spacing) from SeaWinds data is analyzed and some of the limitations of the approach are considered.

II. SCATTEROMETER IMAGING

SeaWinds uses a dual scanning pencil-beam antenna system, making σ^o measurements over a 1800 km wide swath at two nominal incidence angles, 46° (h-pol) and 54.1° (v-pol). The nominal SeaWinds antenna illumination pattern at the surface

is an ellipse. Using range/Doppler filtering, the antenna beam limited footprint is resolved into twelve individual elements (termed ‘slices’), though only 8 are reported in the data products [2]. The slices are approximately 6×25 km. The summed slice measurements are known as ‘egg’ measurements which have an effective size of approximately 25×32 km. Egg measurements are used in 25 km resolution wind retrieval reported in the JPL SeaWinds L2B wind product.

The pulse timing, coupled with antenna rotation, results in a dense spatial sampling of the surface by the slices, with significant measurement response overlap. This dense ‘oversampling’, along with the non-ideal roll-off of the spatial measurement response, is exploited by reconstruction and resolution enhancement algorithms to produce enhanced resolution images of the surface σ^o . The results are σ^o images with finer resolution than the intrinsic resolution of a single slice measurement [1]. The tradeoff in the approach is increased noise. In averaging the slice σ^o into eggs prior to wind retrieval, the L2B product minimizes the noise in the wind estimate. This averaging is lost when using the slices separately with a further noise penalty due to the noise enhancement that accompanies the resolution enhancement/reconstruction.

Previous scatterometers have required multiple passes over the target area to obtain sampling sufficiently dense to benefit significantly from resolution enhancement. (Resolution enhancement algorithms depend on the number of measurements and their spatial sampling of the surface with greater numbers contributing to reduced noise and improved resolution, thereby trading temporal resolution for spatial resolution [3].) While multiple passes are still desired for optimal application to SeaWinds, the dense SeaWinds sampling permits resolution enhancement for single pass data, though the resolution enhancement capability is more limited and noisy.

In past application scatterometer resolution enhancement algorithms have assumed an isotropic response by ignoring any azimuth dependence of the measurements [3]. However, wind retrieval requires azimuth diversity in the σ^o measurements. Further, multiple passes preclude wind retrieval due to the temporal variability of ocean winds. By eliminating the need for multiple passes and by separately processing the various azimuth look directions and incidence angle/polarization combinations of the SeaWinds data, single-pass enhanced resolution σ^o images preserve the azimuth diversity of the original measurements (at a cost of reduced resolution enhancement).

For resolution enhancement the Scatterometer Image Reconstruction (SIR) or AVE algorithms can be used [1], [3]. However, due to reduced computational requirements the AVE algorithm is used in this paper. The AVE algorithm has more limited enhancement capability than SIR, but also tends to be less noisy [3]. Over most of the swath four separate σ^o values can be computed: h-pol fore and aft azimuth looks and v-pol fore

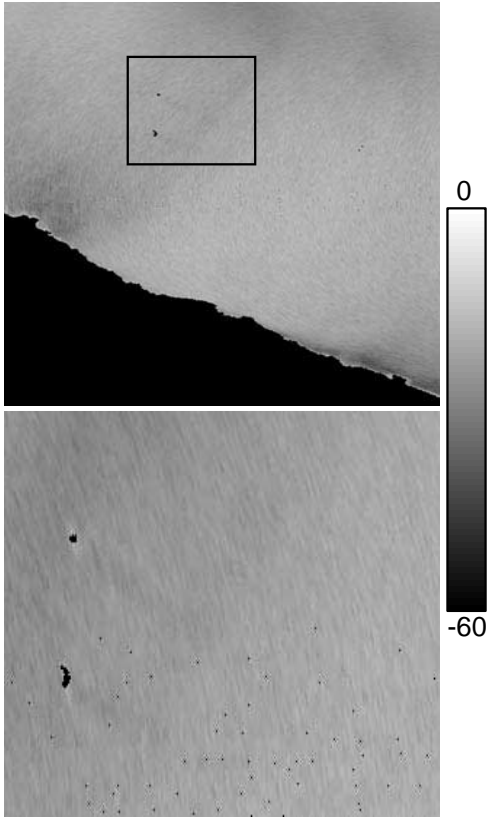


Fig. 1. AVE-derived 2.5 km pixel resolution σ^o (in dB) for SeaWinds v-polarization, fore-look derived from rev 1252 (15 Sept. 1999). (top) Full study area (1800 km \times 1800 km). Lower black area is the west coast of Chile. (bottom) Close view (500 km \times 750 km) around the Juan Fernandez Islands west of Santiago, Chile. The vertical direction corresponds to SeaWinds cross-track with north approximately to the right. Islands and pixels without σ^o measurements are black. Black dots in the lower image are pixels not covered in the sampling. Texture is due to mesoscale variability in the wind and σ^o measurement noise. Note the wind shadows visible as faint dark streaks extending to the right of the islands.

and aft azimuth looks. Over the outer edges of the swath only v-pol measurements are available. The σ^o fields for each case are separately computed from the raw σ^o measurements using the individually varying spatial responses of the measurements and the AVE algorithm. A sample high resolution σ^o field is illustrated in Fig. 1.

The σ^o images are produced on a rectangular along-track/cross-track grid with a pixel size of 2.5 km. In using the AVE algorithm to compute the σ^o image, the spatial response function of each individual slice is required to compute the weighted pixel value estimate. Experience suggests that a minimum pixel sampling of two pixels per slice width is required; thus the nominal pixel size of 2.5 km in order to correspond with a minimum slice width of 5 km. While the SeaWinds measurement geometry generally provides multiple measurement overlap, at some pixel locations the sampling geometry results in inadequate sampling and/or coverage, prohibiting computation of σ^o estimates. Such pixels usually occur in narrow cross-track pixel ranges. The sample timing, spatial response functions, and grid sizes for future instrument designs could be

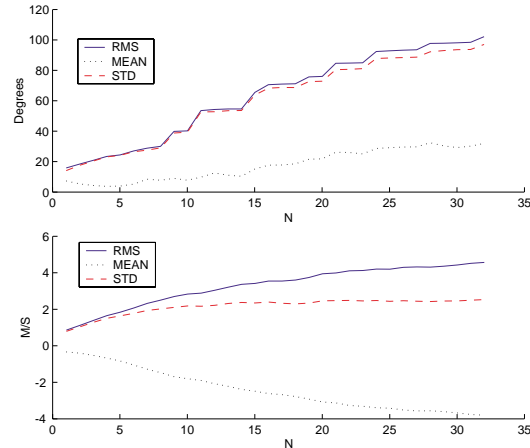


Fig. 2. Monte Carlo estimates of wind direction (top) and speed (bottom) error as a function of the segmentation count of SeaWinds egg σ^o measurements for a true wind of 7 m/s at 42° in the swath ‘sweet spot’.

optimized to avoid this problem.

III. OPERATIONAL HURRICANE MONITORING

Currently, high resolution σ^o fields are being operationally used to support hurricane monitoring. High resolution σ^o images are produced in near-real-time for each SeaWinds orbit. Even without wind retrieval, the enhanced resolution σ^o fields can be an important tool in severe storm forecasting. The fundamental principle on which scatterometry is based is the measurement of σ^o of the wind-roughened surface. While it requires specialized skill to directly interpret ocean surface σ^o fields, the symmetry and low wind speed central eye of hurricanes make such features easy to identify and track (see [4]). Incorporating eye locations derived from high resolution σ^o images improves tracking accuracy.

IV. WIND RETRIEVAL

In computing the AVE σ^o image the azimuth and incidence angle at each pixel is also determined. The wind is then retrieved at each pixel using a standard SeaWinds wind retrieval algorithm. The result at each pixel is from one to four “ambiguities” having similar wind speeds, but differing directions. For these initial experiments ambiguity selection is based on choosing the ambiguity closest (in the vector magnitude difference sense) to the closest selected L2B ambiguity. For pixels with missing σ^o measurements, the wind speed can be estimated but the wind direction estimate accuracy is poor. The accuracy of the wind estimate is also adversely affected by high rain, which is often associated with high winds.

Since the high resolution σ^o values are noisier than the egg values normally used to retrieve the wind, the high resolution wind estimates tend to be significantly noisier than L2B winds and exhibit direction and speed biases. To evaluate the accuracy of the wind retrieval, Monte Carlo simulation is used. Figure 2 illustrates wind accuracy “compass” simulation results as a function of the resolution enhancement of the nominal σ^o measurements. Here, N represents the number of spatial subelements the egg σ^o is divided (or segmented) into. Slices correspond to $N = 8$ while an ideal 2.5 km resolution pixel is

$N \approx 32$, though the actual effective resolution is less than this. As the resolution is enhanced, the noise increases along with the wind speed and direction error. There is thus a tradeoff between wind measurement accuracy and resolution. Of course, this is not surprising. SeaWinds was designed for 25 km resolution wind estimate and we are exceeding its original design specifications. Nevertheless, with caution many applications can tolerate the increased noise for improved resolution.

For a further evaluation, high resolution wind estimates are compared to 25 km resolution L2B winds. A study area (see Fig. 1) was selected which has a range of winds (6-14 m/s) and avoids rain. While the wind direction and speed are fairly uniform in the study area (see Figs. 3-4) interesting mesoscale wind features (e.g., wind shadows) are visible. We note that the high resolution wind speed field suggests the presence of von Karman vortices downwind of the upper island. In Fig. 4 the 25 km grids containing land are blacked out while the high resolution winds are retrieved over each pixel, including land which shows up as high speeds. The 'star' artifact around the upper island is a result of the limited sampling in the resolution enhancement.

As suggested by the simulation results, the wind direction estimates tend to be very noisy. While the estimated wind speed fields always appear consistent, missing σ^0 measurements and poor azimuth geometry combine to occasionally produce poor wind direction estimates at certain cross-track bands. In these bands the direction estimates are poor and are ignored in statistical analysis below. The difference between the selected high resolution wind and L2B wind is determined and statistics computed. The root-mean-square (RMS) wind speed difference over the whole study region is 1.62 m/s with a mean speed difference of 0.43 m/s. Restricting the comparison to the cross-track band corresponding to the small study area the RMS wind speed difference is reduced to 1.15 m/s with a 0.73 m/s bias. In this same area the RMS wind direction difference is 53.7° with a mean bias of 17.6° .

CONCLUSION

Though originally designed to measure vector winds over the ocean at 25 km resolution, SeaWinds can retrieve vector winds at higher resolution, albeit with reduced accuracy. The high resolution winds are not suitable for all applications due to the high noise level but may have application in the study of near-coastal and mesoscale winds. Validation of the high resolution wind estimates is continuing.

REFERENCES

- [1] D.S. Early and D.G. Long, "Image Reconstruction and Enhanced Resolution Imaging from Irregular Samples," *IEEE Trans. Geosci. Remote Sens.*, vol. 39, no. 2, pp. 291-302, 2001.
- [2] M.W. Spencer, C. Wu, and D.G. Long, "Improved Resolution Backscatter Measurements with the SeaWinds Pencil-Beam Scatterometer," *IEEE Trans. Geosci. Remote Sens.*, vol. 38, no. 1, pp. 89-104, 2000.
- [3] D.G. Long, P.J. Hardin, and P.T. Whiting, "Resolution Enhancement of Spaceborne Scatterometer Data," *IEEE Trans. Geosci. Remote Sens.*, vol. 31, no. 3, pp. 700-715, 1993.
- [4] D.G. Long, "High Resolution Wind Retrieval from SeaWinds," *Proc. IGARSS 2001*, pp. 2187-2189, Sydney, Australia, 9-13 July 2001.

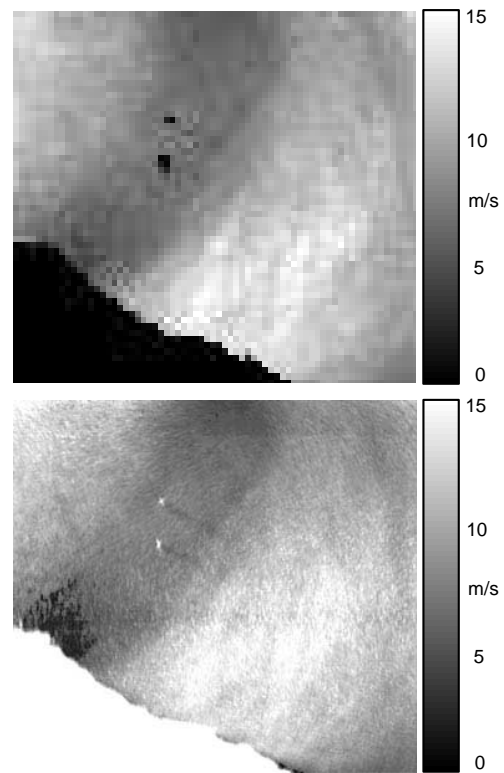


Fig. 3. Images of wind speed in study area. Black area is west coast of Chile. (top) 25 km SeaWinds L2B. (bottom) 2.5 km high resolution wind estimates.

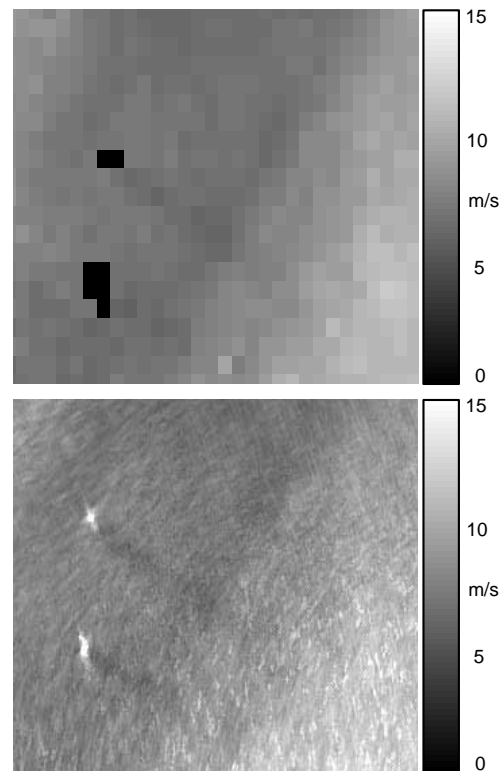


Fig. 4. Images of wind speed in small study area. (top) 25 km SeaWinds L2B. (bottom) 2.5 km high resolution wind estimates.